An Application of Control Volume Method to Simulation of Soil Water Distribution under Line Source of Trickle Emitters

Cong, Vu Chi
Department of Bioproduction Environmental Sciences, Graduate School of Bioresource and Bioenvironmental Sciences, Kyushu University

Tuan, Nguyen Van
Department of Bioproduction Environmental Sciences, Faculty of Agriculture, Kyushu University

Mori, Ken
Department of Bioproduction Environmental Sciences, Faculty of Agriculture, Kyushu University

Hirai, Yasumaru
Department of Bioproduction Environmental Sciences, Faculty of Agriculture, Kyushu University

https://doi.org/10.5109/10098

出版情報：九州大学大学院農学研究院紀要. 53 (1), pp.233-240, 2008-02-28. Faculty of Agriculture, Kyushu University
バージョン：
権利関係：

J. Fac. Agr., Kyushu Univ., **53** (1), 233–240 (2008)

An Application of Control Volume Method to Simulation of Soil Water Distribution under Line Source of Trickle Emitters

Vu Chi CONG[1], Nguyen Van TUAN, Ken MORI* and Yasumaru HIRAI

Laboratory of Bioproduction and Environment Information Sciences, Division of Bioproduction and Environment Information Sciences, Department of Bioproduction and Environmental Science, Faculty of Agriculture, Kyushu University, Fukuoka 812–8581, Japan
(*Received November 9, 2007 and accepted November 30, 2007*)

A method is presented for time variant extent of wetting front and wetting volume that was developed in soil in response to infiltration from surface line source. This method is based on control volume solution of Richard's equation for orthogonal coordination. In control volume method by using implicit scheme, grid size and time of calculated domain can be arbitrarily drawn out. By advantages of simple discretization equation, rapidly performed calculation, direct result of volumetric water content values for various types of soil could be given out. Sand and referenced GILAT sandy loam, PIMA clay were taken to study. Calculated results of vertical infiltration from soil types were verified from referenced paper's result. There's a good agreement between calculated results and the paper's results by using GILAT loamy sand and PIMA clay.

Keywords: line source, trickle emitter, control volume method, wetting front, wetting volume, wetting depth, soil water infiltration

INTRODUCTION

Drip irrigation has been taken interest in various research as well as in conducting experiment with purpose of saving water in arid zone. Simulation of water infiltration in soils has also been taken care by various studies in predicting wetting front and wetting volume in order to optimize parameters for drip irrigation design.

Healy and Warrick (1988) was successful on a simulation of soil water infiltration from surface point source by using finite difference method with a dimensionless form of Richard's equation. From this paper, empirical equation was obtained for simulating soil water distribution. But still, it's rather complicated because of the dimensionless results. The real value of water content must be scaled after calculating process.

Analytical models generally involve in steady state or transient line source or point source infiltration (A. N. Angeakis, 1993; Phillip, 1971; Warrick, 1974) were also successful in simulating water infiltration but with various assumption such as non–ponding surface condition, steady state flow and/or exponential relationship between pressure head and hydraulic conductivity to enable linearization of the Kirchoff equation.

In this report, an application of control volume method to soil water simulation was introduced, utilizing its advantages. The model was counted on the accuracy of wetting front treatment for horizontal infiltration from soil surface with various wide range of soil (represented by the relationship between diffusivity, hydraulic conductivity and volumetric water content).

[1] Laboratory of Bioproduction and Environmental Information Sciences, Division of Bioproduction and Environment Sciences, Department of Bioproduction Environmental Sciences, Graduate School of Bioresource and Bioenvironmental Sciences, Kyushu University

* Corresponding author (E–mail: moriken@bpes.kyushu–u.ac.jp)

THEORIES

Physical model The two–dimensional physical model was described in figure 1. Trickle irrigation is applied on the soil surface, from in–line emitters with constant discharge which can be considered as a horizontal line source by line width of Rs(0) (initial wetting front).

Mathematical bases of model Richard's equation and Darcy principle for saturated–unsaturated soil.

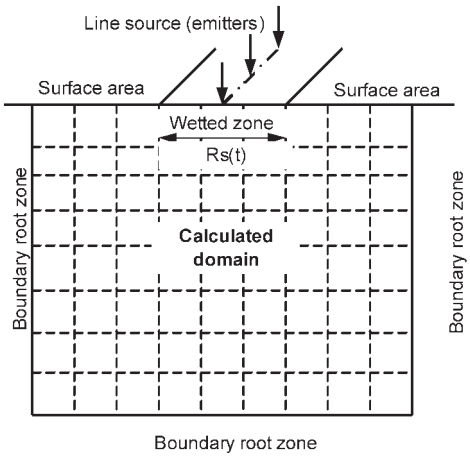

Fig. 1. Two–dimensional–physical model.

Governing equation Following mathematical model of mass conservation, Richard's equation is combined with Darcy's law of flux for saturated–unsaturated soil for 2 dimensions:

$$\frac{\partial \theta}{\partial t} = \frac{\partial}{\partial x}(D_x \frac{\partial \theta}{\partial x}) + \frac{\partial}{\partial z}(D_z \frac{\partial \theta}{\partial z}) - \frac{\partial K}{\partial z} \qquad (1)$$

Where: θ Volumetric water content (L^3/L^3)

x, z are components of orthogonal coordination with z axis is positive downward.

D_x, D_z are soil water diffusivity along the x and z

axis respectively.

K: Unsaturated hydraulic conductivity

t: Elapsed time

Assumptions

– Soil property is isotropic and homogeneous, then $D_x=D_z=D$

– Source term as root water uptake, water evaporation and soil temperature are neglected.

– Pressure head $H=h+z+\pi$. But in equation, osmotic pressure head (counting on absorption by solution and other chemical substance) is also neglected. As consequence, $H=h+z$

Initial and boundary condition

Initial condition

Distribution of volume metric water content at initial time, before irrigating will be assumed to be uniform.

$\theta(x, z, t = 0) = \theta_0$,

Boundary conditions 2 stages of boundary condition were applied:

In order to reach the reality, boundary condition will be divided into 2 stages:

Stage 1: water infiltrates into soil directly from emitter with a discharge q_0 through the initial wetting front $Rs(0)$. Soil will be wetted from initial dryness to saturation within the initial wetting front.

Stage 2: After the time t_1, because normally q_0 exceeds the infiltration's capacity of the soil, the initial zone $Rs(0)$ quickly becomes saturated. A fine layer of water will be established and expands along the time. The wetting front will increase.

Boundary condition for the first stage

a1. At the soil surface

By assuming model without rainfall and no soil water evaporation, condition of soil surface within wetted zone $Rs(0)$ will be described as:

$$q=-D\frac{\partial\theta}{\partial z}=q_0 \quad (z=0,\ x\in Rs(0),\ 0\le t\le t_1,\ q_0 \text{ is input discharge})$$

$$q=0 \quad (z=0,\ x\notin Rs(0),\ 0\le t\le t_1)$$

Other parameters are already explained above.

b1. At other sides of calculated domain: (2 sides and bottom)

Assumption: Volumetric water content values are unchanged along 2 sides and bottom of the calculated domain. Conditions will be described as:

$$\frac{\partial\theta}{\partial x}=0 \quad (x=0 \text{ or } x=x_L,\ 0\le t\le t_1,\ z>0)$$

$$\frac{\partial\theta}{\partial z}=0 \quad (z=z_L,\ 0\le t\le t_1)$$

Boundary condition for the second stage

a2. At the soil surface

At this time ($t>t_1$), wetting front $Rs\ (t)$ will expand by the time. With an assumption that the fine depth water of the soil surface is negligible, condition becomes:

$$\theta=\theta_S \quad (z=0,\ x\in Rs(t),\ t>t_1)$$

$$q=0 \quad (z=0,\ x\notin Rs\ (t),\ t>t_1)$$

b2. At other sides of calculated domain (2 sides and bottom)

Assumption: Volumetric water content values are also unchanged along 2 sides and bottom of the calculated domain. Conditions become :

$$\frac{\partial\theta}{\partial x}=0 \ (x=0 \text{ or } x=x_L,\ t>t_1,\ z>0) \qquad \frac{\partial\theta}{\partial z}=0 \ (z=z_L,\ t>t_1)$$

The wetting front treatment

At this stage, an additional condition will be applied as a water balance principle to describe the size of wetting front at soil surface $Rs(t)$:

Principle: Total amount of water applied to the soil

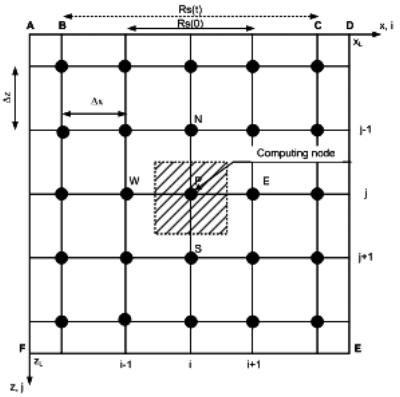

Fig. 2. Control volume scheme.

from emitter is equal to total amount of infiltrated water into the soil. At the infiltrated volume of soil, real value of infiltrated water at each volume ($dx\times dz\times 1$) can be considered as $\frac{\theta}{1+\theta}\times dx\times dz$. Therefore, mathematical equation becomes:

$$qt=\iint_{\Omega}\left[\left(\frac{\theta}{1+\theta}\right)_t-\left(\frac{\theta}{1+\theta}\right)_{t=0}\right]dxdz \qquad (2)$$

(Ω: Infiltration zone, t: calculated time)

Numerical solution Using control volume method (Fig. 2) with implicit scheme, TDMA (Tri–diagonal matrix algorithm) application with a small adjustment of Gauss–Seidel line by line iteration.

General discretization from governing equation (1) becomes:

$$\alpha_P\theta_P=\alpha_W\theta_W+\alpha_E\theta_E+\alpha_N\theta_N+\alpha_S\theta_S+\alpha_P^0\theta_P^0+S_{source} \qquad (3)$$

Where: $\alpha_P=\alpha_W+\alpha_E+\alpha_N+\alpha_S+\alpha_P^0$. These coefficients at calculated grid points were described in Fig. 2 and Table 1 or Table 2.

S_{Source}: represents for capillary conductivity components in the discretization equation.

In order to utilize TDMA algorithm, equation (3) was changed into: $-a_W\theta_W+a_P\theta_P-a_E\theta_E=d$

Where θ_W, θ_P, θ_E: variables which are need to be calculated. All coefficients of (2) were calculated as in the table

Table 1. Coefficients for the first boundary condition

Position in the calculated domain	Coefficients of discretization equation					
	a_W	a_E	a_N	a_S	a_P^0	d
AB	$\frac{\Delta z}{2\Delta x}D_w$	$\frac{\Delta z}{2\Delta x}D_e$	0	$\frac{\Delta x}{\Delta z}D_s$	$\frac{\Delta x\Delta z}{2\Delta t}$	$a_S\theta_S+a_P^0\theta_P^0-\Delta xK_s$
BC	$\frac{\Delta z}{2\Delta x}D_w$	$\frac{\Delta z}{2\Delta x}D_e$	0	$\frac{\Delta x}{\Delta z}D_s$	$\frac{\Delta x\Delta z}{2\Delta t}$	$a_S\theta_S+a_P^0\theta_P^0-\Delta xK_s+q_0\Delta x$
CD	$\frac{\Delta z}{2\Delta x}D_w$	$\frac{\Delta z}{2\Delta x}D_e$	0	$\frac{\Delta x}{\Delta z}D_s$	$\frac{\Delta x\Delta z}{2\Delta t}$	$a_S\theta_S+a_P^0\theta_P^0-\Delta xK_s$
DE	$\frac{\Delta z}{\Delta x}D_w$	0	$\frac{\Delta x}{2\Delta z}D_n$	$\frac{\Delta x}{2\Delta z}D_s$	$\frac{\Delta x\Delta z}{2\Delta t}$	$a_N\theta_N+a_S\theta_S+a_P^0\theta_P^0+\frac{\Delta x}{2}(K_n-K_S)$
EF	$\frac{\Delta z}{2\Delta x}D_w$	$\frac{\Delta z}{2\Delta x}D_e$	$\frac{\Delta x}{\Delta z}D_n$	0	$\frac{\Delta x\Delta z}{2\Delta t}$	$a_N\theta_N+a_P^0\theta_P^0-\Delta xK_n$
FA	0	$\frac{\Delta z}{\Delta x}D_e$	$\frac{\Delta x}{2\Delta z}D_n$	$\frac{\Delta x}{2\Delta z}D_s$	$\frac{\Delta x\Delta z}{2\Delta t}$	$a_N\theta_N+a_S\theta_S+a_P^0\theta_P^0+\frac{\Delta x}{2}(K_n-K_S)$
A	0	$\frac{\Delta z}{\Delta x}D_e$	0	$\frac{\Delta x}{\Delta z}D_s$	$\frac{\Delta x\Delta z}{2\Delta t}$	$a_S\theta_S+a_P^0\theta_P^0-\Delta xK_s$
D	$\frac{\Delta z}{\Delta x}D_w$	0	0	$\frac{\Delta x}{\Delta z}D_s$	$\frac{\Delta x\Delta z}{2\Delta t}$	$a_S\theta_S+a_P^0\theta_P^0-\Delta xK_s$
E	$\frac{\Delta z}{\Delta x}D_w$	0	$\frac{\Delta x}{\Delta z}D_n$	0	$\frac{\Delta x\Delta z}{2\Delta t}$	$a_N\theta_N+a_P^0\theta_P^0+\Delta xK_n$
F	0	$\frac{\Delta z}{\Delta x}D_E$	$\frac{\Delta x}{\Delta z}D_n$	0	$\frac{\Delta x\Delta z}{2\Delta t}$	$a_N\theta_N+a_P^0\theta_P^0+\Delta xK_n$
Internal points	$\frac{\Delta z}{\Delta x}D_w$	$\frac{\Delta z}{\Delta x}D_E$	$\frac{\Delta x}{\Delta z}D_n$	$\frac{\Delta x}{\Delta z}D_s$	$\frac{\Delta x\Delta z}{\Delta t}$	$a_N\theta_N+a_S\theta_S+a_P^0\theta_P^0+\Delta x(K_n-K_S)$

Table 2. Coefficients for the second boundary condition

Position in the calculated domain	Coefficients of discretization equation					
	a_W	a_E	a_N	a_S	a_P^0	d
AB	$\frac{\Delta z}{2\Delta x}D_w$	$\frac{\Delta z}{2\Delta x}D_e$	0	$\frac{\Delta x}{\Delta z}D_s$	$\frac{\Delta x\Delta z}{2\Delta t}$	$a_S\theta_S+a_P^0\theta_P^0-\Delta xK_s$
CD	$\frac{\Delta z}{2\Delta x}D_w$	$\frac{\Delta z}{2\Delta x}D_e$	0	$\frac{\Delta x}{\Delta z}D_s$	$\frac{\Delta x\Delta z}{2\Delta t}$	$a_S\theta_S+a_P^0\theta_P^0-\Delta xK_s$
DE	$\frac{\Delta z}{\Delta x}D_w$	0	$\frac{\Delta x}{2\Delta z}D_n$	$\frac{\Delta x}{2\Delta z}D_s$	$\frac{\Delta x\Delta z}{2\Delta t}$	$a_N\theta_N+a_S\theta_S+a_P^0\theta_P^0+\frac{\Delta x}{2}(K_n-K_S)$
EF	$\frac{\Delta z}{2\Delta x}D_w$	$\frac{\Delta z}{2\Delta x}D_e$	$\frac{\Delta x}{\Delta z}D_n$	0	$\frac{\Delta x\Delta z}{2\Delta t}$	$a_N\theta_N+a_P^0\theta_P^0-\Delta xK_n$
FA	0	$\frac{\Delta z}{\Delta x}D_e$	$\frac{\Delta x}{2\Delta z}D_n$	$\frac{\Delta x}{2\Delta z}D_s$	$\frac{\Delta x\Delta z}{2\Delta t}$	$a_N\theta_N+a_S\theta_S+a_P^0\theta_P^0+\frac{\Delta x}{2}(K_n-K_S)$
A	0	$\frac{\Delta z}{\Delta x}D_e$	0	$\frac{\Delta x}{\Delta z}D_s$	$\frac{\Delta x\Delta z}{2\Delta t}$	$a_S\theta_S+a_P^0\theta_P^0-\Delta xK_s$
D	$\frac{\Delta z}{\Delta x}D_w$	0	0	$\frac{\Delta x}{\Delta z}D_s$	$\frac{\Delta x\Delta z}{2\Delta t}$	$a_S\theta_S+a_P^0\theta_P^0-\Delta xK_s$
E	$\frac{\Delta z}{\Delta x}D_w$	0	$\frac{\Delta x}{\Delta z}D_n$	0	$\frac{\Delta x\Delta z}{2\Delta t}$	$a_N\theta_N+a_P^0\theta_P^0+\Delta xK_n$
F	0	$\frac{\Delta z}{\Delta x}D_E$	$\frac{\Delta x}{\Delta z}D_n$	0	$\frac{\Delta x\Delta z}{2\Delta t}$	$a_N\theta_N+a_P^0\theta_P^0+\Delta xK_n$
Internal points	$\frac{\Delta z}{\Delta x}D_w$	$\frac{\Delta z}{\Delta x}D_E$	$\frac{\Delta x}{\Delta z}D_n$	$\frac{\Delta x}{\Delta z}D_s$	$\frac{\Delta x\Delta z}{\Delta t}$	$a_N\theta_N+a_S\theta_S+a_P^0\theta_P^0+\Delta x(K_n-K_S)$

1 and table 2. Coefficients D and K at grid point E, W, S, N, P were calculated by using central different scheme.

TRIALS AND DISCUSSIONS

By taking reference from St. Elmaloglou & N. Malamos 2003, two types of soil were carried out: GILAT sandy loam, a loamy soil containing 48% sand and 20% clay described by Bresler *et al*. (1971) and PIMA clay loam, a clay loam soil described by Stockon and Warrick (1971). The two soils are different in hydrodynamic characteristic (capillary conductivity and diffusivity) and soil textures (porosity, percentage of sand).

Input data of the relationship between capillary conductivity and volumetric water content, diffusivity and volumetric water content were calculated from this paper as following formulas:

$$\theta(h)=\theta_r+\frac{\theta_S-\theta_r}{[1+(\alpha h)^n]^m} \qquad K(h)=K_S e^{a_0 h}$$

$$D=\frac{K}{\left(\frac{d\theta}{dh}\right)}$$

$$\frac{d\theta}{dh}=\frac{\alpha.m.n(\theta_S-\theta_r)\ (-\alpha h)^{(n-1)}}{[1+(\alpha h)^n]^{m+1}}$$

Where: θ_r: residual volumetric water content (cm^3/cm^3)
θ_S: saturated volumetric water content (cm^3/cm^3)
h: soil water potential (cm)
K_s: saturated hydraulic conductivity (cm/min.)
α, a_0, m, n: empirical coefficients

Table 3. Physical parameters of two referenced soil types

Parameters	Type of soil		Unit
	GILAT sandy Loam	PIMA Clay loam	
m	0.677	0.220	–
n	3.097	1.282	–
α	0.016	0.032	1/cm
a_0	0.044	0.020	1/cm
K_s	0.875	0.413	cm/h
θ_s	0.440	0.550	cm^3/cm^3
θ_r	0.120	0.200	cm^3/cm^3

In addition, fine sand was analyzed, using Bruce & Klute method and pF experiment to find out the relationship between diffusivity, capillary conductivity and volumetric water content. Those relationships were described in Fig. 3.

Input data

For two referenced types of soil, domain foundation was 180 cm in horizontal direction and 100 cm in vertical direction. Grid size was generated by 1 cm in each direction. Time step was 10 to 30 minutes with total calculated time was 10 to 16 hours. Discharge was variously supplied by 4.0, 5.0, 6.0 (l/m/h) for PIMA clay loam and 4.0, 6.0, 8.0 (l/m/h) for GILAT sandy loam, respectively. Initial volumetric water content is 0.1244 (cm^3/cm^3) for GILAT sandy loam and 0.322 (cm^3/cm^3) for PIMA clay loam.

For experimented fine sand, domain is 60 cm×60 cm along the two directions, with grid size was 1 cm×1 cm respectively. Time step was 1 minute and total calculation time was 60 minutes. Discharge input and initial θ were 20 (l/m/h) and 0.006 (cm^3/cm^3) respectively.

Calculation convergence Trial running program for the above mentioned types of soil. Calculation process has stability by variance of time. In the model, Gauss Seidel line by line iteration was used but with a little modification of under relaxation number. This iteration algorithm is famously used for computational fluid dynamics and water/material temperature in which, diffusion and conductivity are gradually changed by temperature, water velocity or water density increment. (Steven C. Chapra, 1997). But in case of soil physics, various types of soil give various forms of $D(\theta)$ and $K(\theta)$. From sand to clay, the non–linear of $D(\theta) \sim \theta$ property becomes stronger. In case of PIMA clay soil, with only small change of θ near saturated state causes huge difference of diffusivity value (when θ from 0.5342 to 0.5491 (cm^3/cm^3) then $D(\theta)$ from 3.164 to 5.7 (cm/min.) for PIMA clay, when θ from 0.4333 to 0.439 (cm^3/cm^3) then $D(\theta)$ from 5.963 to 37.945 (cm/min.) for GILAT sandy loam and see figure 3 for fine sand). Therefore, re–calculation of θ by using the previous iteration θ value in general did not show convergence (except the sample as mentioned fine sand). Because of being not

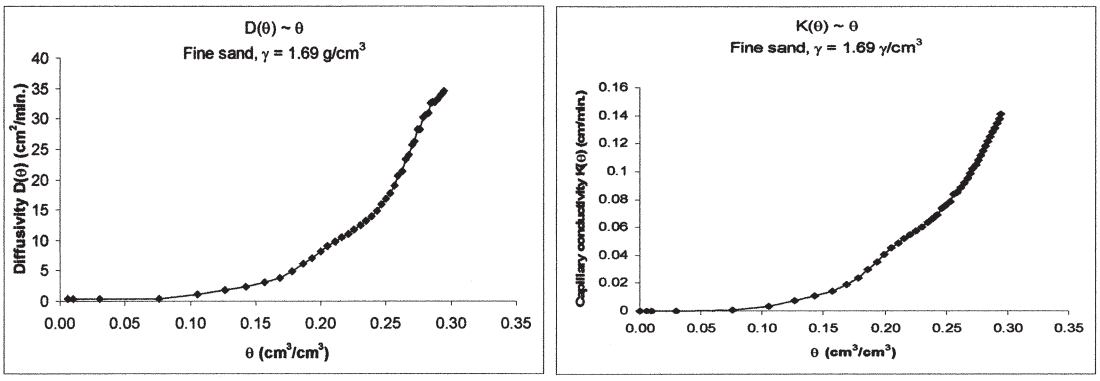

Fig. 3. Physical properties of fine sand.

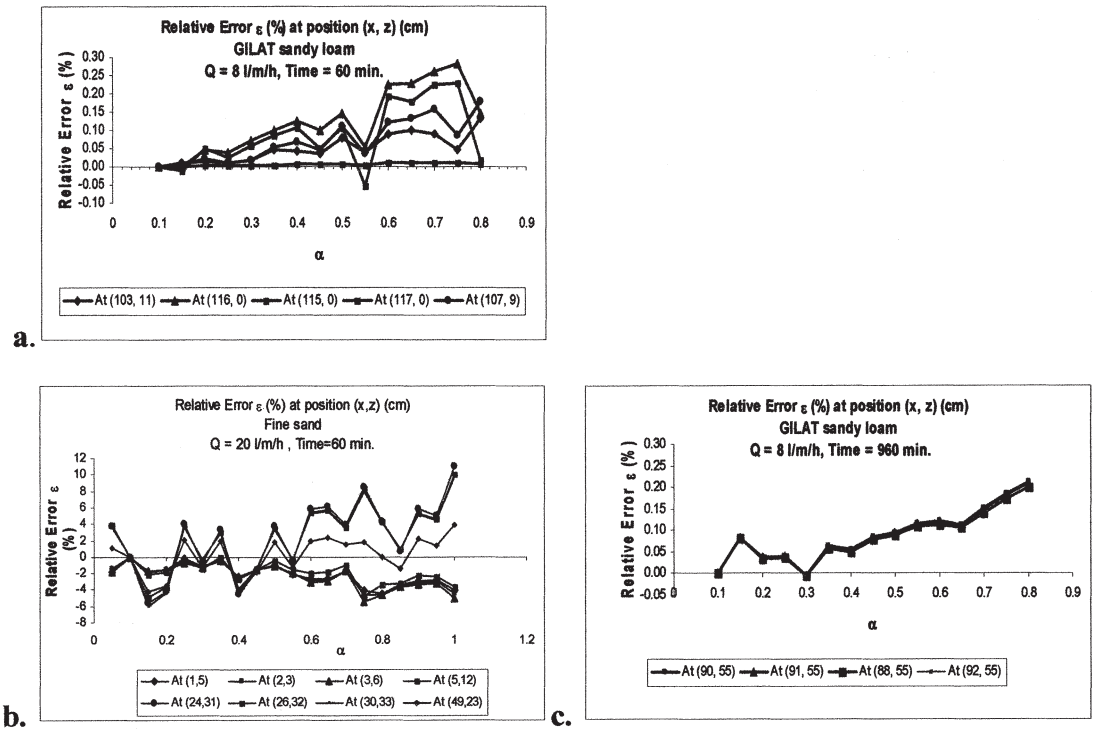

Fig. 4. Relative errors ε at various α (case: a, b and c).

small enough grid size and the sudden change of diffusivity value in the range of θ and hence the slowness of water soil infiltration, a small modification of iteration process was proposed in this model.

$$\theta_{i,j,k}=\theta^*_{i,j,k}+\alpha(\theta_{i,j,k}-\theta^*_{i,j,k}) \quad (4)$$

$\theta_{i,j,k}$: Calculated value of $\theta(x, z, t)$; $\theta^*_{i,j,k}$: Assumption value of $\theta(x, z, t)$ at previous iteration. $\alpha\in(0.0, 1.0]$: Under relaxation number. When α=1.0, iteration process is the same as in normal Gauss Seidel line by line method.

By changing under relaxation number α (from 0.05 to 1.0 for fine sand, from 0.1 to 0.8 for GILAT sandy loam) from θ values at previous iterations which are applied to new iteration process (see equation 4), convergence was successful.

Iteration process couldn't get convergence if applying α>0.8 for GILAT sandy loam, but sand. Trial running was set up for testing maximum relative error of volumetric water content of all grid points in the domain at estimated time with various α by 0.05 step value increments (Fig. 4).

$$\varepsilon=\frac{\theta^*(x, z, t)_{\alpha=0.1}-\theta^*(x, z, t)\alpha_i}{\theta^*(x, z, t)_{\alpha=0.1}}\times 100$$

Where: α_i = 0.05, 0.1, ..1.0

θ^*(x, z, t): Maximum of θ(x, z, t) in the calculated domain at each value of α

ε(%): Relative error of θ at grid point in the calculated domain.

In Fig. 4, process of calculating ε was applied to some positions (x, z) in the calculated domain in which, ε series are in the range of highest and lowest values. In general, maximum ε of all above shown–α were just 0.28% and 0.29% for GILAT sandy loam at time of 60 minutes and 960 minutes, respectively but up to 11.06% in case of sand at time of 60 minutes. From Fig. 4 for three types of soil it can be seen that, the closer α value reached 1.0 (or 0.8), the higher ε value had at the calculated grid points. These relative errors ε do show the stability of convergent iteration and believable algorithm. Anyway, the best application of under relaxation number α applied in the model depends on each type of soil and can be determined only when soil water distribution experiment is conducted (real θ value will be compared with calculated θ value).

Comparison of vertical depths infiltration between calculated results and the reference

By applying α=0.35, sample data from three soil types was carried out to calculate water infiltration. Results were described in Fig. 5, 6, 7 and 8. Vertical depths infiltration of GILAT sandy loam and PIMA clay were calculated as shown in Fig. 5. Calculated results can be compared between empirical equation proposed by St. Elmaloglou & N. Malamos, 2003: $V=dT^c$ (cm) (with parameters d and c was shown in Table 4, T is time (hour), V is vertical depth of infiltration) and calculated values from this model. Calculated wetting depth in the model was assumed at positions in which $\theta=1.25\theta_0$. There was slight difference between the two results, especially in case of PIMA clay. Maximum relative errors of wetting depth between the two results (Fig. 5) were

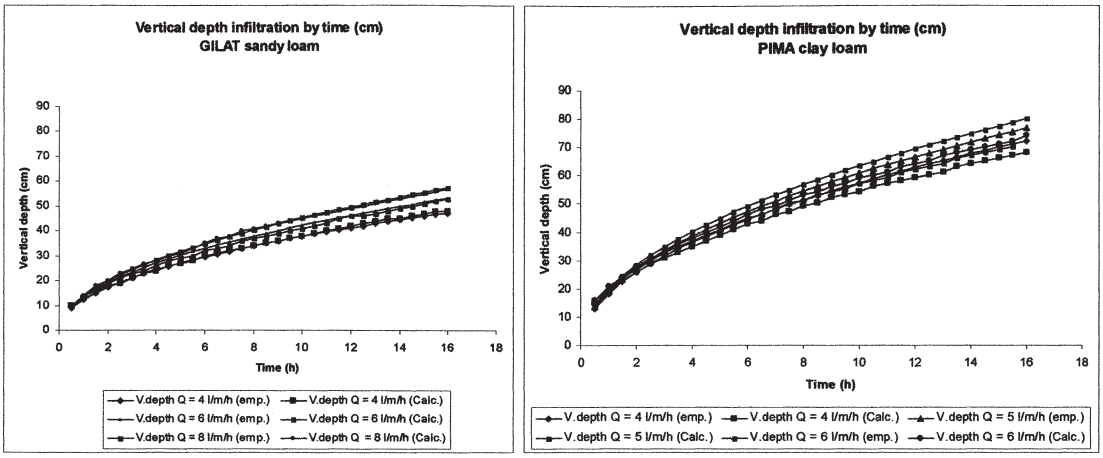

Fig. 5. Vertical infiltration comparison between calculated program and referenced paper result.
Cal.: value calculated from program; **emp**.: value calculated from empirical equation in referenced paper

5.4% (0.6 cm in difference at time of 3.5 h when Q=6 l/m/h was applied) in case of GILAT loamy sand, 8.5% (6.7 cm in difference at time of 15.5 h when Q=6 l/m/h was applied) in case of PIMA clay.

It might be that because of additional source/sink application (root water uptake) from referenced paper, rounded value of wetting–depth–position, under relaxation number θ and especially, little difference of initial α applied between the model and referenced paper, but in general the trend of wetting–depth development is reasonably agreement.

Wetting front

In reality, input discharge usually exceeds the infiltration capacity of soil, especially loam and clay by elapsed time. In addition to natural infiltration in horizontal direction, the remained water will spread out to make soil at surface layer saturated. Because of no other water–losses assumptions except infiltration, water conservation principle should be applied to define the size of saturated zone *R(t)* by time as described in the equation 2. Water conservation at each time–iteration was reviewed to define the size *Rs(t)* of saturated zone. Wetting front increment had stability for all of three soil types. At one type of soil (Fig. 6), the increment of discharge intensity caused increment of wetting front.

Table 4. Parameters of empirical equation in referenced paper

Parameters	GILAT sandy loam		PIMA clay loam	
	d	c	d	c
Q=4 (l/m/h)	12.540	0.480	18.360	0.494
Q=5	–	–	19.400	0.496
Q=6	13.770	0.488	20.200	0.496
Q=8	14.090	0.507	–	–

In Fig. 6, it is clear that there was a remarkable surface wetting front difference between two types of soil. Big changes of discharge input (4.0, 6.0 and 8.0 (l/m/h) in case of GILAT sandy loam) caused not so much different values of wetting front *Rs(t)* and in general, wetting fronts of GILAT sandy loam are much smaller than in case of PIMA clay.

Water infiltration, especially vertical infiltration capacity of one soil type depends on not only diffusivity but also capillary conductivity. Fig. 7 shows calculation results from three soil types data, in which input data from PIMA clay and GILAT sandy loam had the same calculation time (10 hours), the same irrigation intensity

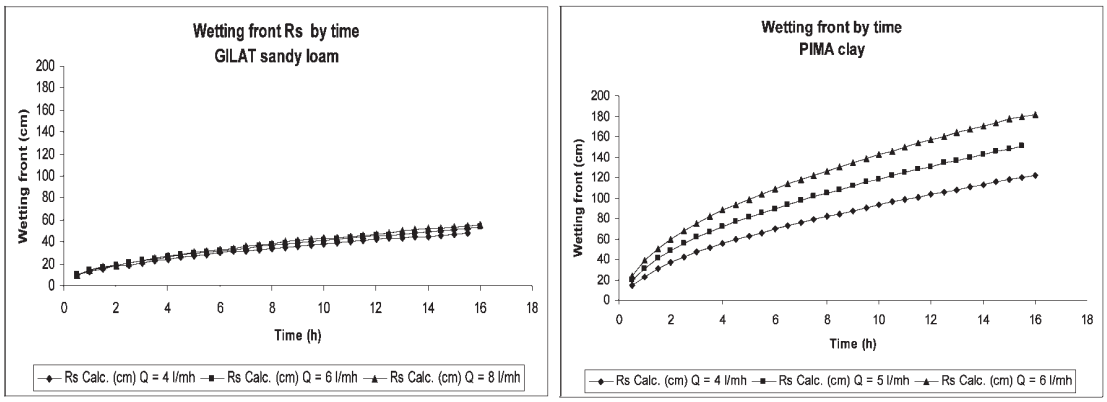

Fig. 6. Horizontal wetting front from calculated program.

q=4.0 (l/m/h) and the same grid size 100 cm×180 cm. Data input from sand was different because infiltration capacity at time 10 hours after irrigating was too large in comparison to 180 cm×100 cm domain size. It can be seen that, shapes of wetting volumes are different among the three soil types. In the fine sand, wetting volume had nearly circle wetting volume but eliptic shape in the GILAT sandy loam while it was longer eliptic in PIMA clay. The difference did not only appear in shape but also in θ value distribution. Near grid points which had θ_0 values, there was sudden change of θ values along distance in case of PIMA clay (from 0.4 down to θ_0=0.322) and GILAT sandy loam (0.2 down to θ_0=0.1244), not like in case of fine sand (gradually changed from 0.2 down to 0.006).

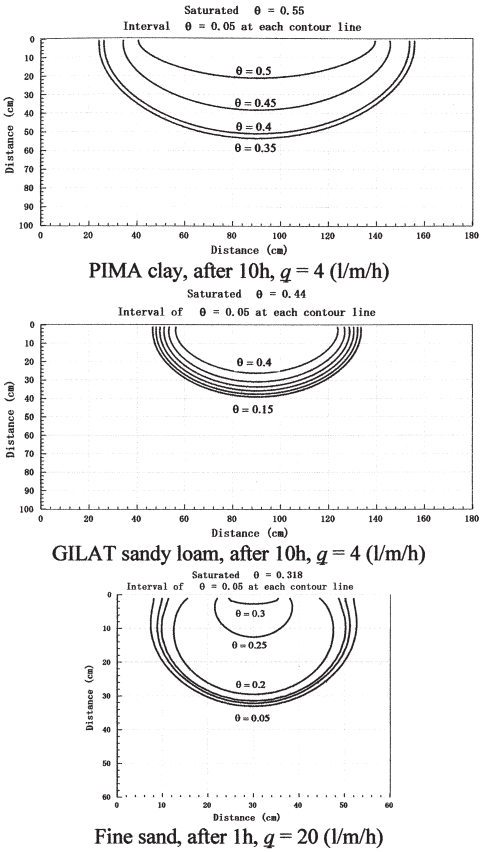

Fig. 7. Difference of wetting volume and $\theta(x, z, t)$ distribution at different soil types θ unit: (cm^3/cm^3).

Because of soil physical properties (smaller diffusivity, smaller capillary conductivity by series of θ) and soil texture (higher porosity), wetting fronts at soil surface of PIMA clay increase faster than those in GILAT sandy loam and wetting volumes also increase faster than those from GILAT sandy loam by time increment. Fine sand had the smallest value of wetting front but the largest value of wetting depth in comparison at the same input discharge and time after irrigation.

Testing program was carried out for GILAT sandy loam with (180 cm×100 cm) domain size and input discharge of 6 l/m/h at time of 1 h, 5 h, 10 h and 16 h after starting irrigation. It is understandable that there is a relationship between wetting–depth and wetting front at soil surface. Increasing wetting front causes wetting–depth development. Case of GILAT sandy loam in Fig. 8 showed that, after the time of 1 h, 5 h, 10 h and 16 h, wetting front increased at 14 cm, 29 cm, 41 cm, 53 cm and wetting depth increased at 13 cm, 27 cm, 38 cm and 48 cm. This can be concluded that calculated results from the model in Fig. 8 showed logical evidence of wetting volume development thus, had good tendency to the reality.

Wetting fronts and wetting depths can be arbitrarily chosen at positions in which, θ values changed from 0.4 (cm^3/cm^3) to 0.15 (cm^3/cm^3) or minor. Visually, wetting depth can be seen at some levels of θ values thus, θ should be measured by experiment (i.e. Bruce & Klute method) to estimate the accuracy of wetting volume in this model.

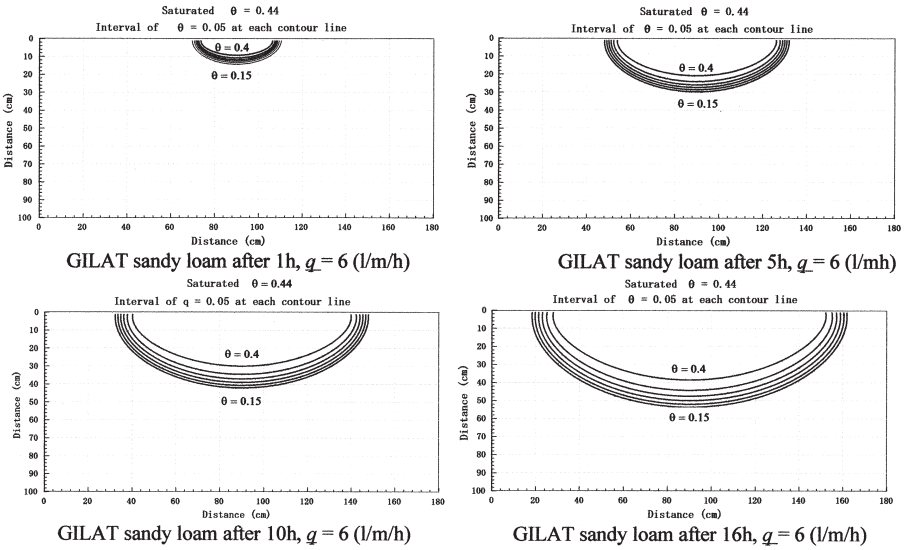

Fig. 8. Wetting volume development and $\theta(x, z, t)$ distribution by elapsed time with the same input discharge. Case of GILAT sandy loam. θ unit: (cm^3/cm^3)

CONCLUSION

A model with application of control volume method to simulation of soil water distribution under line source initially based on referenced sample results of GILAT sandy loam and PIMA clay has some important features and notices as following:

1. The two–stage boundary condition is necessary for implementation and reaches the reality because at initial time, soil surface at irrigated zone must be gradually wetted to saturated water soil state. If only first condition was used, at sometime θ exceeds saturated value and iteration process was broken, leading to unstable and unacceptable results. When only second condition was applied, it means that soil surface at irrigated zone suddenly becomes saturated (the same meaning as wetting volume at time $t<t_1$ will be eliminated) therefore it can not adapt the reality.

2. Wetting front at soil surface was calculated simply and directly based on total water volume conservation, reflecting a real physical phenomenon. By using small step increment of wetting front assumption (Rs) for wetting front iteration, error between the amount of water application and the amount of infiltrated water will be minimized at each calculated time. The size of wetting front should be checked by experiment. Anyway, calculated results from this model could be precise at some level of discharge input because a fine layer of water on soil surface was eliminated.

3. Although the model was applied by simple assumptions: uniform initial θ, homogeneous soil, elimination of evaporation and source/sink term (root water uptake), an elimination of water layer at soil surface and just a few of sample trials but it can give a good tendency for numerical analysis of soil water infiltration when those above obstacles will be surpassed.

4. When successfully applying a modification of Gauss Seidel line by line iteration (applying under relaxation number), control volume method could be a good solution for simulation of soil water infiltration because of its advantages: less time consumption (applying Tri–diagonal algorithm), gains accurate calculated values at not only large number of grid points but also large grid size.

REFERENCES

Angelakis A. N. 1993 *Time–dependent soil–water distribution under a circular trickle source.* Water Resources management **7**: 225–235

Bruce R. R. & A. Klute, 1956 *The measurement of soil moisture diffusivity. Soil science society proceeding* 458–462

Bresler E, Heller J, Diner N, Ben–Asher J, Brandt A, Goldberg D 1971 *Infiltration from a trickle source, II. Experimental data and theoretical predictions.* Soil Sci. Soc. Am. Pro. **35**: 683–689

Don Kirkham, W. K. Powers. *Advanced soil physics,* Wiley Interscience, 1972

Elmaloglou St. and N. Malamos. 2003 *A method to estimate soil–water movement under a trickle surface line source, with water extraction by roots.* Irrig. and Drain. **52**: 273–284 (2003)

Fredie R. Lamm, James E. Ayars, Francis S. Nakayama. *Micro Irrigation for crop production – design, operation an management*, Elsevier, 2007

Gabriela Marinoschi. *Functional approach to nonlinear models for water flow in soils.* Springer, 2006

Healy R. W. and A. W. Warrick, 1988 *A generalized solution to infiltration from a surface point source.* Soil Sci. Soc. Am. J. **52**: 1245–1251

Philip J. R. 1971 *General theorem on steady infiltration from surface sources with application to point and line source.* Soil. Sci. Soc. Am. Proc. **35**: 867–871

Steven C. Chapra. *Surface water quality modeling*, Mc Graw–Hill, 1997

Stockton JG, Warrick AW. 1971 *Spatial variability of unsaturated hydraulic conductivity.* Soil Sci. Soc. Am. Pro. **35**: 847–848

Suhas V. Patankar, *Numerical heat transfer and fluid flow*, Taylor & Francis. 1980

Tsuyoshi Miyazaki. *Water flow in soils*, Taylor & Francis, 2006

Van Genuchten M. Th. 1980 *A closed–form equation for predicting the hydraulic conductivity of unsaturated soil.* Soil Sci. Soc. Am. J. **44**: 892–898

Versteeg H. K. & W. Malalasekera. *An introduction to computational fluid dynamics – The finite volume method*, Longman Scientific & technical. 1995

Warrick A. W. 1974 *Time dependent linearized infiltration. I. Point sources.* Soil. Sci. Soc. Am. Proc. Vol. 38